An N-Terminal Three-Helix Fragment of the Exchangeable Insect Apolipoprotein Apolipophorin III Conserves the Lipid Binding Properties of Wild-Type Protein†

Matthias Dettloff,‡ Paul M. M. Weers,§ Marc Niere,‡ Cyril M. Kay,|| Robert O. Ryan,§ and Andreas Wiesner*,‡

Institute of Biology/Zoology, Free University of Berlin, Königin-Luise-Strasse 1-3, D-14 195 Berlin, Germany, Children's Hospital Oakland Research Institute, Oakland, California 94609, and Protein Engineering Network of Centres of Excellence (PENCE), Department of Biochemistry, University of Alberta, Edmonton, Alberta T6G 2S2, Canada

Received June 16, 2000; Revised Manuscript Received November 27, 2000

ABSTRACT: Apolipophorin III (apoLp-III) from the greater wax moth *Galleria mellonella* is an exchangeable insect apolipoprotein that consists of five amphipathic α-helices, sharing high sequence identity with apoLp-III from the sphinx moth *Manduca sexta* whose structure is available. To define the minimal requirement for apoLp-III structural stability and function, a C-terminal truncated apoLp-III encompassing residues 1−91 of this 163 amino acid protein was designed. Far-UV circular dichroism spectroscopy revealed apoLp-III(1−91) has 50% α-helix secondary structure content in buffer (wild-type apoLp-III 86%), increasing to essentially 100% upon interactions with dimyristoylphosphatidylcholine (DMPC). Guanidine hydrochloride denaturation studies revealed similar stability properties for wild-type apoLp-III and apoLp-III(1−91). Resistance to denaturation for both proteins increased substantially upon association with phospholipid. In the absence of lipid, wild-type apoLp-III was monomeric whereas apoLp-III(1−91) partly formed dimers and trimers. Discoidal apoLp-III(1−91)−DMPC complexes were smaller in diameter (13.5 nm) compared to wild-type apoLp-III (17.7 nm), and more molecules of apoLp-III(1−91) associated with the complexes. Lipid interaction revealed that apoLp-III(1−91) binds to modified spherical lipoprotein surfaces and efficiently transforms phospholipid vesicles into discoidal complexes. Thus, the first three helices of *G. mellonella* apoLp-III contain the basic features required for maintenance of the structural integrity of the entire protein.

Apolipophorin III (apoLp-III)[1] is an abundant exchangeable apolipoprotein involved in lipid transport and metabolism in insects. Like human apolipoprotein (apo) E, apoA-I, and apoC, it is comprised of amphipathic α-helices and associates reversibly with circulating lipoproteins. ApoLp-III from the greater wax moth *Galleria mellonella* is a 163 residue protein with a molecular mass of 18 076 Da, sharing high amino acid sequence identity with apoLp-III from other lepidopteran insects (*1*, *2*). The role of apoLp-III in lipid transport is well understood (see *3*−*6* for reviews). During energy-demanding activities, such as flight, several insect species are known to mobilize diacylglycerol (DG) from fat body tissue. In adult insects, DG is loaded onto preexisting high-density lipophorin particles (HDLp), with concomitant association of up to 16 molecules of apoLp-III, resulting in the formation of low-density lipophorin (LDLp). LDLp particles release their neutral glycerolipid load at flight muscle cells without internalization. Depletion of DG results in dissociation of apoLp-III and regeneration of HDLp. Free apoLp-III generated can be reused for another cycle of DG transport. Aside from its role in lipid transport, recent reports indicate an involvement of apoLp-III in other physiological processes including immune activation (*1*, *7*−*8*), programmed cell death (*9*), detoxification (*10*), and hemagglutination (*11*). For a better understanding of apoLp-III function in these processes, detailed knowledge about its structural and functional properties is necessary.

High-resolution structures are available for lipid-free apoLp-III from *Locusta migratoria* (*12*) and *Manduca sexta* (*13*). NMR studies with *M. sexta* apoLp-III, which shares a 71% amino acid sequence identity with apoLp-III from *G. mellonella* (*2*), revealed that the lipid-free protein consists of a bundle of five amphipathic α-helices connected by short loops (*13*). Hydrophobic residues orient toward the interior of the helix bundle, whereas hydrophilic residues face the aqueous environment. Biophysical and functional data suggest that during lipid association, apoLp-III undergoes a conformational opening about "hinged" loops that connect helical segments in the bundle. Opening of the helix bundle exposes the hydrophobic interior of the protein, which becomes available for interaction with lipoprotein surface defects (*12*−*17*). While the loops between helix-2 and helix-3 and between helix-4 and helix-5 act as hinges, the other loops

† Supported by grants from the Deutsche Forschungsgemeinschaft (DFG WI 1612/1, A.W.), National Institutes of Health (HL 64159, R.O.R.), Friedrich-Ebert-Stiftung (scholarship to M.D.), and Sonnenfeld-Stiftung (scholarship to M.N.).

* To whom correspondence should be addressed. Phone: ++49-30-838-53937; fax: ++49-30-838-53916; email: awiesner@zedat.fu-berlin.de.

‡ Free University of Berlin.

§ Children's Hospital Oakland Research Institute.

|| University of Alberta.

[1] Abbreviations: apo, apolipoprotein; apoLp-III, apolipophorin III; CD, circular dichroism; DG, diacylglycerol; DMPC, dimyristoylphosphatidylcholine; DMPG, dimyristoylphosphatidylglycerol; DMS, dimethyl suberimidate; LDL, low-density lipoprotein; PL-C, phospholipase C; SDS−PAGE, sodium dodecyl sulfate−polyacrylamide gel electrophoresis; TFE, trifluoroethanol.

10.1021/bi0013804 CCC: $20.00
Published on Web 02/15/2001

are believed to initiate contact to the lipid surface (*18*, *19*). The structure of apoLp-III isolated from unrelated insect species is conserved since the X-ray structure of *L. migratoria* apoLp-III shows a similar molecular architecture, despite low sequence identity (*12*).

Previous studies with fragments of apoLp-III revealed that individual helices or two connected helical segments together are insufficient to retain either the structure or the function of apoLp-III (*20*−*22*). To further evaluate the minimal structural requirements for apoLp-III structural and/or functional properties, we have engineered a C-terminal deletion mutant composed of the three N-terminal helical segments (residues 1−91). ApoLp-III(1−91) adopts α-helical secondary structure and retains properties of the intact protein. The truncated apolipoprotein spontaneously transforms DMPC bilayer vesicles into discoidal complexes and forms a stable binding interaction with modified human low-density lipoprotein.

MATERIALS AND METHODS

Design of Mutant. The nucleotide sequence encoding residues 1−91 of *G. mellonella* apoLp-III was PCR-amplified from a full-length cDNA template (*7*) with *Pfu* polymerase (Stratagene). The following oligonucleotide primers were employed: 5′-CCG ACG CGT CCA CGC CGC TGC AG-3′ and 5′-CGG AAT TCT TAG TGC GCG CGC CGC AGC TCC TC-3′. The phosphorylated amplification product was digested with *Eco*RI and ligated into the pET 22b+ vector (Novagen) via its *Msc*I and *Eco*RI sites and transformed into *Escherichia coli* BL 21 (DE3) cells. The DNA sequence was verified by cycle sequencing following evaluation with an automated DNA sequencer (Licor 4000L, MWG-Biotech).

Expression and Purification of Recombinant Proteins. Expression and purification of recombinant apoLp-III was performed as previously outlined (*7*, *23*). Briefly, 25 mL of an overnight culture of *E. coli* BL21 (DE3) cells (grown in 2 × yeast tryptone medium at 30 °C) harboring the *G. mellonella* wild-type apoLp-III/pET or apoLp-III(1−91)/pET plasmid was added to 1 L of M9 minimal media supplemented with 13.3 mM glucose, 0.1 mM $CaCl_2$, 2 mM $MgSO_4$ and grown at 37 °C to an OD_{600} = 0.6. Isopropyl-β-D-thiogalactopyranoside was added to a final concentration of 2 mM, and culture continued for 4 h at 30 °C. Subsequently, the cells were pelleted by centrifugation, and the supernatant, concentrated by ultrafiltration, was subjected to Sephadex G75 gel filtration chromatography and reversed-phase high-performance chromatography (RP-HPLC). The purity of the samples was analyzed by analytical RP-HPLC and sodium dodecyl sulfate−polyacrylamide gel electrophoresis (SDS−PAGE) using 4−20% acrylamide gradient gels (*24*). Gels were stained with Coomassie Blue. The correct size of the deletion mutant was verified by electrospray mass spectrometry (VG quattro mass spectrometer, Fisons Instruments, Manchester, U.K.).

Hydrodynamic Studies. Fringe counts were performed using a Beckman XLI analytical ultracentrifuge and double-sector capillary synthetic boundary sample cells as described (*25*). Prior to ultracentrifugation, samples were dialyzed for 48 h in 50 mM sodium phosphate, pH 7.0. The absorbance of each sample was measured using 1.0 cm path length cuvettes. Samples (120 μL) were loaded into one sector of the sample cell, and 400 μL of the dialysate was loaded into the other sector. Runs were performed at 8000 rpm, and scans were taken when fringes were resolved across the boundary region between protein solution and solvent. The number of fringes produced across the boundary was measured and converted to concentration using an average increment of 3.31 fringes mg^{-1} mL^{-1}.

Sedimentation equilibrium experiments were carried out at 20 °C using interference optics. Aliquots of sample (110 μL) were loaded into 6-sector CFE cells, allowing three concentrations of sample to be run simultaneously. Runs were performed at 18 000, 22 000, 26 000, and 30 000 rpm, and each speed was maintained until there was no significant difference in scans taken 2 h apart to ensure equilibrium was achieved. The sedimentation equilibrium data were evaluated with the NonLin analysis program using a nonlinear least-squares curve-fitting algorithm (*26*). The program Sednterp was employed to calculate the partial specific volume of the proteins from the amino acid compositions using the method of Cohn and Edsall (*27*).

Circular Dichroism Spectroscopy. Circular dichroism (CD) spectroscopy was performed in a JASCO J-720 spectropolarimeter calibrated with a 0.06% solution of ammonium *d*-camphor-10-sulfonate. The temperature in the sample chamber was maintained using a Lauda RM6 low-temperature circulator. Data were collected using the J700 for Windows standard analysis software, version 1.10.00. Prior to measuring ellipticity at 221 nm, samples treated with guanidine hydrochloride were incubated for 24 h. CD spectra were analyzed for secondary structure by a modified Contin program by Provencher and Glöckner (*28*), using poly-L-glutamate as standard for the calculation of the α-helical content of the proteins.

Preparation of Protein−DMPC Complexes. Dimyristoylphosphatidylcholine (DMPC) or dimyristoylphosphatidylglycerol (DMPG) vesicles were prepared by dissolving the phospholipids in chloroform/methanol 3:1 (v/v). The solvent was evaporated to dryness under a stream of N_2, resulting in a thin film of dry lipid. Buffer (20 mM Tris-HCl, 150 mM NaCl, 0.5 mM EDTA, pH 7.2) was added to a final concentration of 10 mg of lipid/mL, heated to 42 °C, and vigorously vortexed for 1 min. From this solution, unilamellar vesicles were prepared by extrusion using 200 nm filters (Avanti Polar Lipids) (*29*). To 5 mg of unilamellar DMPC vesicles was added 2 mg of apoLp-III or apoLp-III-(1−91), mixed, and incubated overnight at 24 °C. KBr (1.12 g) was added to the cleared solution, and the volume was adjusted to 2.5 mL. The samples were transferred to 5 mL Quick seal tubes, overlayed with 0.9% NaCl, and centrifuged at 65 000 rpm for 2 h at 4 °C in a VTi 65.2 rotor. The gradient was fractionated into 500 μL aliquots and measured for protein using the bicinchoninic acid protein assay (Pierce). Fractions containing protein−lipid complexes were dialyzed against phosphate-buffered saline (154 mM NaCl, 50 mM NaH_2PO_4, 50 mM Na_2HPO_4, 3.4 mM EDTA, pH 7.0). Aliquots of the preparations were subjected to native PAGE. For guanidine hydrochloride denaturation studies, the complexes were dialyzed against 50 mM sodium phosphate (pH 7.2) for 48 h.

Electron Microscopy. Protein−lipid complexes were adsorbed to hydrophilized, carbon-coated grids and rinsed 3 times with buffer (10 mM Tris, 10 mM NaCl, 1.5 mM

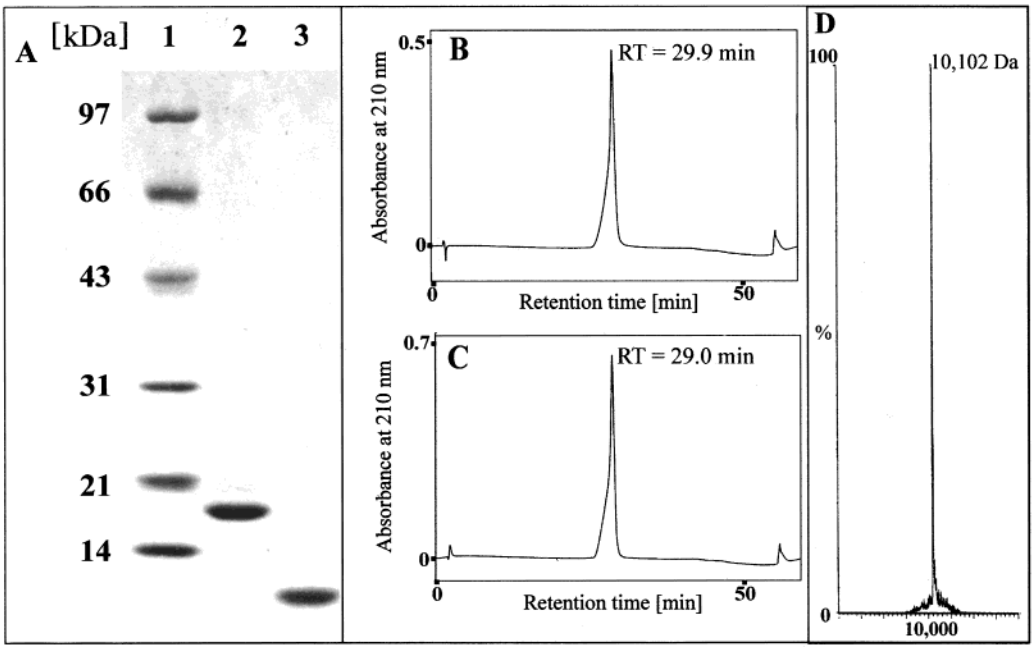

FIGURE 1: Expression of wild-type and apoLp-III(1−91). Panel A: SDS−PAGE (4−20% slab) of wild-type apoLp-III (lane 2) and apoLp-III(1−91) (lane 3). Lane 1: Marker proteins. Panels B and C: HPLC profiles of wild-type (B) and apoLp-III(1−91) (C). Panel D: Mass spectrometry of apoLp-III(1−91).

$MgCl_2$). The grids were then negatively stained for 10 s with 2% sodium phosphotungstate, pH 7.0. Photographs were taken in a Philips EM 420 operated at 100 kV.

Cross-Linking Studies. Chemical cross-linking was performed as described previously (*17*). Wild-type or truncated apoLp-III−DMPC discoidal complexes (50 μg of protein) were incubated at room temperature for 3 h with increasing concentrations of dimethyl suberimidate (DMS), ranging from 0.2 to 2 mM. DMS was dissolved in 1 M triethanolamine (pH 9.7), resulting in a final triethanolamine concentration of 0.1 M. The reaction was terminated by addition of SDS−PAGE sample treatment buffer; the samples were boiled for 5 min and loaded onto an 8−20% acrylamide SDS−PAGE gel.

Vesicle Clearance Assay. The rate of apoLp-III-induced transformation of phospholipid vesicles into protein−lipid complexes was monitored using a Perkin-Elmer spectrofluorometer (model LS 50B) as described (*18*). Excitation and emission wavelengths were set at 612 nm, using a slit width of 3 nm. The temperature of the cuvette holder was maintained at 24 °C. Phospholipid vesicles (250 μg) were equilibrated in vesicle buffer to 24 °C for 5 min. Protein (250 μg for DMPC and 10 μg for DMPG, 1 mL final sample volume) was added and mixed for 10 s. The decrease in light scattering was monitored as a function of time.

LDL Protection Assay. Incubation of human LDL with phospholipase C (PL-C, from *Bacillus cereus*, Sigma, P-7147) was performed as described (*30*, *31*). Fifty micrograms of human LDL protein in 50 mM Tris-HCl, pH 7.5, containing 150 mM NaCl and 2 mM $CaCl_2$ was incubated at 37 °C for 2 h with 160 milliunits of PL-C. Where specified, increasing amounts of wild-type apoLp-III or apoLp-III(1−91) were included in incubations of LDL and PL-C (200 μL final sample volume). The absorbance at 340 nm was measured at the times indicated.

RESULTS

Design, Expression, and Purification of Deletion Mutant. To identify the minimal requirement for maintenance of apoLp-III structural stability and lipid binding, a truncated apoLp-III mutant was designed. Based on the NMR solution structure of *M. sexta* apoLp-III (*8*; PDB code 1MAP), sequence alignment identified the helix boundaries of the first three helices of *G. mellonella* apoLp-III: helix-1 (residues 7−28), helix-2 (residues 35−65), and helix-3 (residues 69−90). Wild-type recombinant *G. mellonella* apoLp-III and the C-terminal deletion mutant containing the first three helical segments, apoLp-III(1−91), were overexpressed in *E. coli*. Remarkably, both recombinant proteins escape the bacteria and accumulate in the culture medium at concentrations up to 100 mg/L, from which apoLp-III was purified. SDS−PAGE analysis revealed a single band with a mass of ∼18 kDa for wild-type apoLp-III and ∼10 kDa for apoLp-III(1−91) (Figure 1A). Analytical HPLC profiles (Figure 1B,C) showed a high degree of purity while mass spectrometry of the deletion mutant gave a single mass of 10 102 ± 2 Da (Figure 1D), identical to that expected on the basis of its amino acid sequence (10 104 Da).

Biophysical Properties. The hydrophobic moment of individual helices in apoLp-III, calculated according to Eisenberg (*32*), did not reveal major differences among the different helices: helix-1 = 0.451, helix-2 = 0.445, helix-3 = 0.542, helix-4 = 0.358, helix-5 = 0.492. Far-UV CD spectra (Figure 2A) revealed a high α-helix content for wild-type apoLp-III (86%), which was not affected by 50% (v/v) trifluoroethanol (TFE, Table 1). ApoLp-III(1−91) had 50% α-helix in buffer alone, while TFE (50% v/v) increased the α-helix content to essentially 100% (Table 1). Interaction with DMPC caused an increase in the α-helix content for both wild-type apoLp-III and apoLp-III(1−91) (Table 1).

The effect of guanidine hydrochloride exposure on the secondary structure content of wild-type apoLp-III and

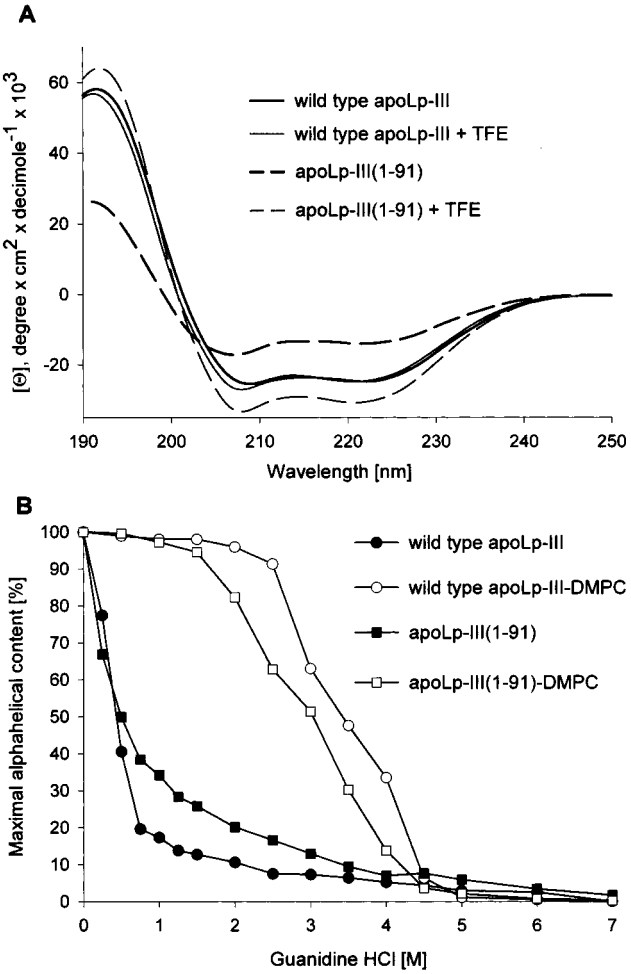

FIGURE 2: Far-UV CD spectra and guanidine hydrochloride induced denaturation of wild-type apoLp-III and apoLp-III(1−91). Panel A: CD spectra of wild-type apoLp-III or apoLp-III(1−91). CD spectra were also recorded in the presence of 50% TFE. Panel B: Denaturation of apoLp-III induced with guanidine hydrochloride of lipid-free and DMPC-bound apoLp-III. Prior to measurement, samples were incubated with different concentrations of guanidine hydrochloride for 24 h.

Table 1: Biophysical Properties of ApoLp-III[a]

	wild-type apoLp-III	apoLp-III(1−91)
α-helix (%)	86	50
α-helix + TFE (%)	86	100
α-helix + DMPC (%)	100	100
[guanidine-HCl]$_{1/2}$ lipid-free (M)	0.3	0.4[b]
[guanidine-HCl]$_{1/2}$ DMPC (M)	3.5	3.0

[a] The percentage of α-helical content was calculated by a modified Contin program by Provencher and Glöckner (*28*) from the far-UV CD spectra of the proteins. [Guanidine-HCl]$_{1/2}$ is the molar concentration of guanidine hydrochloride required to give a 50% decrease in ellipticity at 221 nm. [b] The denaturation midpoint is approximately estimated as the low structure of the peptide did not allow a precise measurement.

apoLp-III(1−91) is shown in Figure 2B. Consistent with data reported for *M. sexta* apoLp-III (*33*) wild-type *G. mellonella* apoLp-III was relatively labile, displaying a denaturation midpoint of 0.3 M. The corresponding value for apoLp-III-(1−91) was 0.4 M. Association with DMPC stabilized both apoLp-III samples as shown by their significantly increased resistance to guanidine hydrochloride induced denaturation (Table 1). The lipid-free wild-type apoLp-III sedimentation

Table 2: Properties of Discoidal Complexes of DMPC and ApoLp-III[a]

	wild-type apoLp-III	apoLp-III(1−91)
particle mass (kDa)	∼700	∼400
diameter (nm)	17.7 ± 1.8	13.5 ± 2.4
no. of apoLp-III	5	7
$t_{1/2}$ (s)	425	80

[a] Particle masses were estimated from native PAGE; the diameters of the disks were measured from electron micrographs (Figure 4). The number of apoLp-III units was determined by cross-linking studies (Figure 5); $t_{1/2}$ represents the time required for a 50% reduction of sample turbidity of a mixture of DMPC vesicles and full-length or apoLp-III(1−91), using a protein:lipid mass ratio of 1:1.

equilibrium data fit well to a single species model with no evidence of association and a calculated apparent molecular mass of 17 030 Da, implying it is monomeric in solution (Figure 3A). The deletion mutant displayed definite evidence of association and fit best to a monomer−dimer model, with an apparent molecular mass of 18 910 Da, although the higher concentration data sets, when fit individually, had an apparent molecular mass slightly higher than dimer, indicating a small amount of higher order species as well (Figure 3B).

Phospholipid−ApoLp-III Complexes. Electron micrographs of apoLp-III−DMPC complexes prepared with wild-type apoLp-III revealed a homogeneous population of discoidal structures (Figure 4). The size and shape of the complexes (Table 2) were similar to those described for *M. sexta* apoLp-III (*17*). ApoLp-III(1−91) also forms discoidal structures, but these are smaller in diameter compared to complexes formed with wild-type apoLp-III. Native PAGE analysis revealed complex sizes of about 700 kDa for wild-type apoLp-III−DMPC disks and about 400 kDa for apoLp-III-(1−91)−DMPC disks (not shown).

Chemical Cross-Linking. To determine the number of apoLp-III molecules bound per disk, apoLp-III−DMPC complexes prepared with wild-type apoLp-III or apoLp-III-(1−91) were incubated with increasing amounts of dimethyl suberimidate (DMS) and analyzed by SDS−PAGE. The data showed up to five wild-type apoLp-III molecules per disk, as indicated by the appearance of bands with molecular masses of 19, 42, 61, 80, and 105 kDa (Figure 5A). Experiments performed at 4 mg/mL DMS did not lead to a further increase in the number of apoLp-III molecules per disk (data not shown). Addition of DMS to lipid-free wild-type apoLp-III showed only the presence of a broad band at ∼20 kDa, which was slightly shifted due to internal cross-linking. This confirms that *G. mellonella* wild-type apoLp-III is present as a soluble monomer in buffer. Complexes of DMPC and apoLp-III(1−91) contained up to seven molecules of truncated apoLp-III per disk as judged by SDS−PAGE (Figure 5B). Cross-linking of the lipid-free deletion mutant showed the presence of internally cross-linked monomers, dimers, and small amounts of trimers (Figure 5B, lane 2).

Phospholipid Vesicle Clearance. A known property of amphipathic exchangeable apolipoproteins is an ability to transform phospholipid vesicles into much smaller discoidal lipid−protein complexes. Wild-type apoLp-III cleared a suspension of DMPC vesicles in about 2000 s, whereas in the absence of apolipoprotein the suspension remained turbid

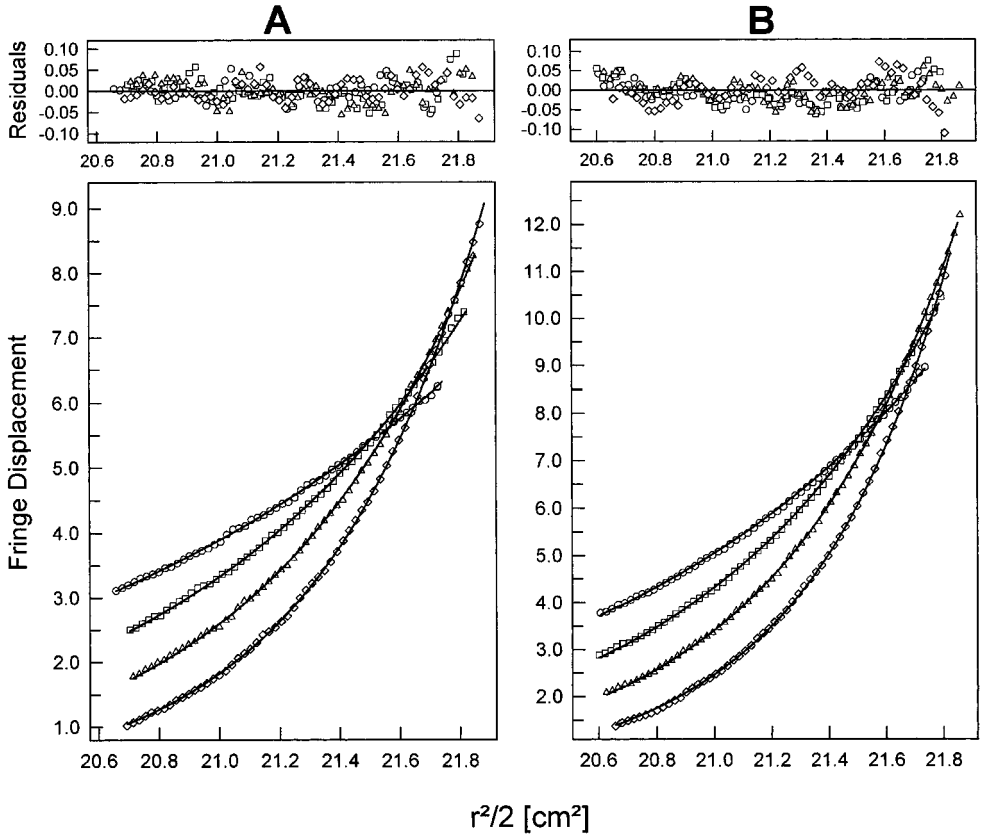

FIGURE 3: Sedimentation equilibrium distribution of apoLp-III. Shown are fits of wild-type apoLp-III (1.42 mg/mL) to a single species model (panel A), and deletion mutant (1.48 mg/mL) to a monomer−dimer model (panel B). Bottom panels show raw data points, and the lines represent the best fits from four speed conditions: 18 000 rpm (circles), 22 000 rpm (squares), 26 000 rpm (triangles), and 30 000 rpm (diamonds). The residuals of the fits are shown in the upper panels.

(Figure 6). Using the same amount of protein mass, apoLp-III(1−91) showed a strongly increased vesicle clearance rate compared to wild-type apoLp-III. The time required to achieve 50% of the maximum clearance ($t_{1/2}$, Table 2) was 425 s for wild-type apoLp-III, and 80 s for apoLp-III(1−91). Using equal molar protein amounts, $t_{1/2}$ for apoLp-III-(1−91) was 85 s (not shown). Thus, apoLp-III(1−91) associated about 5 times faster with DMPC vesicles than wild-type apoLp-III. *G. mellonella* apoLp-III is also able to disrupt dimyristoylphosphatidylglycerol (DMPG) vesicles, a process that occurs at a much faster rate than with DMPC vesicles ($t_{1/2}$ DMPG = 40 s). Clearance rates for apoLp-III-(1−91) were too fast to measure as complete clearance was achieved during mixing (data not shown).

Protection against PL-C-Induced LDL Aggregation. Treatment of human LDL with PL-C results in an aggregation of LDL particles due to the appearance of surface-localized DG. This process can be monitored by an increase in sample turbidity. Exchangeable apolipoproteins are able to prevent aggregation by association with DG patches created on the surface of modified lipoprotein particles (*30*, *31*). This process is specific for exchangeable apolipoproteins since other globular proteins (i.e., bovine serum albumin or carbonic anhydrase) are unable to protect PL-C-treated LDL from aggregation (*34*). Wild-type apoLp-III or apoLp-III-(1−91) prevent PL-C-induced aggregation of LDL to a similar extent. However, when limiting amounts of apoLp-III were used, it was observed that wild-type apoLp-III was more effective than apoLp-III(1−91) in preventing aggregation (Figure 7). The estimated amount of protein sufficient to reach 50% of the maximum turbidity (2 h incubation) was 12.5 μg for wild-type apoLp-III and 24 μg for apoLp-III-(1−91).

DISCUSSION

Structural Studies with ApoLp-III(1−91). The N-terminal 10 kDa fragment (residues 1−91) of *G. mellonella* apoLp-III characterized in this study includes only the first three helices. In contrast to the full-length protein which is present as a monomer, the deletion mutant partly self-associates to form dimers and, to a lesser extent, trimers. Apparently the presence of five α-helices prevents self-association of the protein while removal of two helices favors dimerization. CD measurements revealed that the α-helical content of the deletion mutant is 50%, noticeably lower than wild-type apoLp-III (86%). These results indicate that the deletion mutant does not simply fold as a 3-helix bundle in solution. The α-helix content of apoLp-III(1−91) was induced by TFE (50% v/v) to a maximal extent (100%), and, after binding to DMPC, both proteins were essentially 100% α-helical. This is in agreement with values observed for *M. sexta* apoLp-III (*17*), which also adopts essentially 100% α-helix content upon binding to DMPC.

Wild-type apoLp-III and apoLp-III(1−91) showed guanidine hydrochloride denaturation midpoints of 0.3 and 0.4 M, respectively. These values are similar to that of *L. migratoria* apoLp-III (0.6 M) or *M. sexta* apoLp-III (0.36 M) (*16*, *33*). The relatively low stability of lipid-free apoLp-III may provide a flexible structure to accommodate conformational changes induced by lipoprotein surface interac-

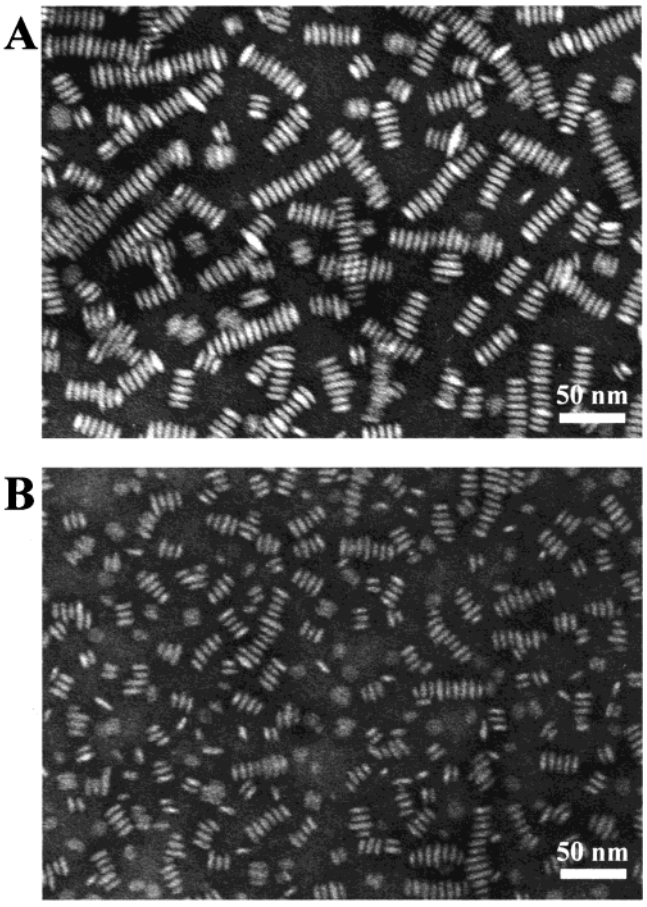

FIGURE 4: Electron micrographs of DMPC−protein complexes. DMPC was complexed with wild-type apoLp-III (panel A) or apoLp-III(1−91) (panel B). Samples were negatively stained with 2% phosphotungstate for electron microscopy.

tions. As reported for the latter apolipoproteins (*16*, *17*), lipid binding causes a significant increase in stability of both wild-type apoLp-III and apoLp-III(1−91).

Lipid Binding Properties of ApoLp-III(1−91). The deletion mutant rapidly associates with unilamellar phospholipid vesicles. The rate of transformation into disklike structures from DMPC and DMPG vesicles was significantly higher than those observed for wild-type apoLp-III. The resulting discoidal complexes were smaller and contained more molecules of apoLp-III(1−91) than complexes made with the full-length protein. Apparently, the smaller size, lower α-helical content, and self-associating properties are no hindrance for the deletion mutant to interact with phospholipid vesicles.

In earlier studies, it has been shown that a complementary charge distribution between protein and the corresponding lipid is important for the initiation of lipid binding (*35*, *36*). Indeed, addition of positively charged residues in the loop regions in *L. migratoria* apoLp-III increased the clearance rates of zwitterionic or anionic phospholipid vesicles (*18*). However, in the present study the change in the relative amount of Arg or Lys introduced by removing two helices from *G. mellonella* apoLp-III is negligible. Cooperative interactions within the peptide or the altered presentation of positively charged residues to the solution environment due to unique folding of the deletion mutant could conceivably explain the enhanced rate of association with DMPC or DMPG vesicles. In addition, because of its decreased

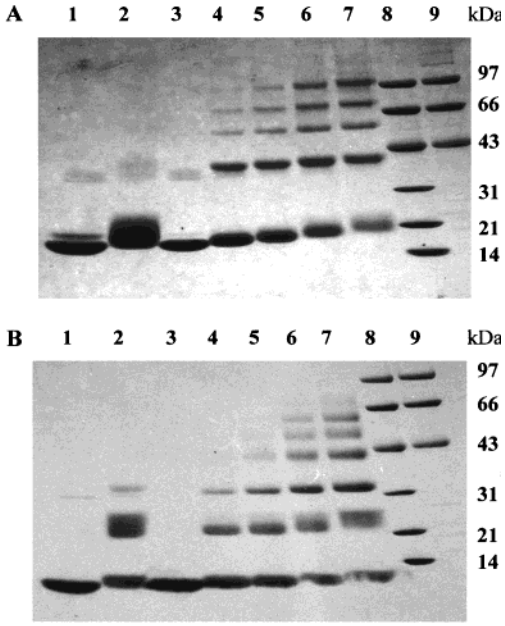

FIGURE 5: SDS−PAGE of wild-type apoLp-III−DMPC and apoLp-III(1−91)−DMPC complexes cross-linked with DMS. Protein−DMPC complexes (50 μg of protein) were incubated with increasing amounts of DMS and analyzed by SDS−PAGE (8−20% slab). Panel A: Wild-type apoLp-III. Panel B: ApoLp-III(1−91). Lane 1, apoLp-III; lane 2, apoLp-III with 2 mg/mL DMS; lane 3, apoLp-III−DMPC complexes; lane 4, apoLp-III−DMPC complexes with 0.2 mg/mL DMS; lane 5, apoLp-III−DMPC complexes with 0.4 mg/mL DMS; lane 6, apoLp-III−DMPC complexes with 1.0 mg/mL DMS; lane 7, apoLp-III−DMPC complexes with 2.0 mg/mL DMS; lanes 8 and 9, molecular mass markers.

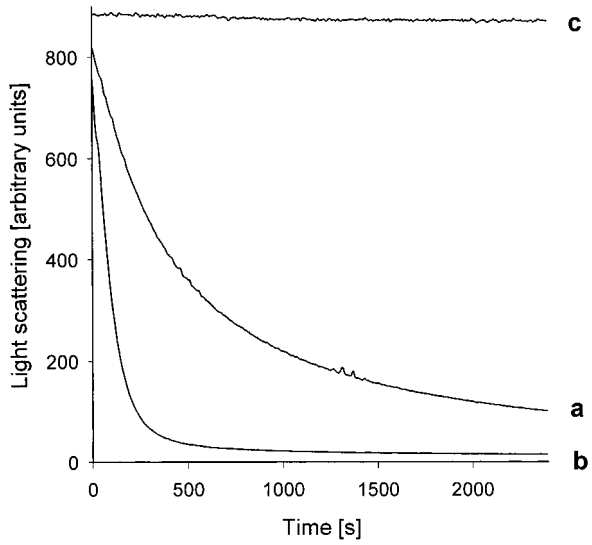

FIGURE 6: Phospholipid vesicle clearance. Mixtures of DMPC vesicles and wild-type apoLp-III (curve a) or apoLp-III(1−91) (curve b) were incubated at a phospholipid:protein mass ratio of 1:1. Vesicle clearance was followed as a function of time at 24 °C by 90° light scattering in a fluorescence spectrophotometer (excitation and emission wavelength set at 612 nm). Curve c corresponds to vesicles only.

resistance to guanidine denaturation compared to wild-type apoLp-III, apoLp-III(1−91) might require less energy to induce a change in structure upon lipid binding, resulting in faster lipid association kinetics. In this context, it is worth mentioning that a decrease in pH from 7 to 4 results in a 40-fold increase in the DMPC clearance rates of *M. sexta* apoLp-III (*37*). This was explained by a partially unfolded

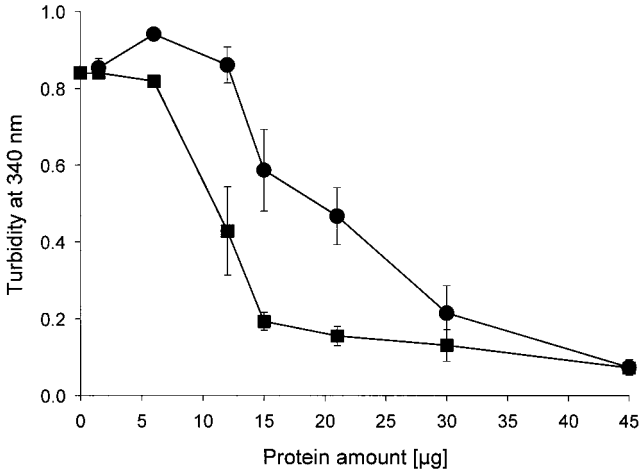

FIGURE 7: Effect of apoLp-III and apoLp-III(1−91) on PL-C-induced turbidity of human LDL. Fifty micrograms of LDL protein was incubated for 2 h at 37 °C with 160 milliunits of PL-C in the presence of different amounts of wild-type apoLp-III (squares) or apoLp-III(1−91) (circles). Sample absorbance was monitored at 340 nm. Error bars represent the standard deviation of three determinations.

state of the protein at low pH (a "molten globule" conformation).

ApoLp-III(1−91) is able to prevent PL-C-induced LDL aggregation. However, higher protein amounts in comparison to wild-type apoLp-III are necessary for complete protection of lipolyzed LDL. This might be a result of removal of the short helix normally located between helix-3 and helix-4 (residues 95−100). It is thought to play an important role in the initiation of lipoprotein binding (*19*). On the other hand, this short helix may not be an absolute requirement for lipid surface recognition of apoLp-III as its function can be replaced by other regions in the protein.

The interaction of apoLp-III with lipoprotein surfaces versus phospholipid vesicles differs fundamentally, and this fact might explain the different outcome of both assays. ApoLp-III penetrates and disrupts vesicle bilayers to form disklike particles (*34*) while binding of apoLp-III to spherical lipoproteins takes place after creation of hydrophobic patches on the LDL surface induced by PL-C. It is worth mentioning that the DG appearance on lipoprotein surfaces is the trigger for apoLp-III binding in vivo (*38*−*40*), suggesting that the results obtained in this assay resemble the physiological function of exchangeable insect apolipoproteins.

Concluding Remarks. Studies with synthetic peptides revealed that several factors are important with regard to the lipid binding abilities of peptides forming amphipathic helices (*41*, *42*), i.e., the number of helices involved (*43*), cooperativity between helices (*44*, *45*), and the amphipathicity of the peptide (*35*, *46*). Cleavage of *L. migratoria* apoLp-III in the middle of helix-3 yielded two 9K fragments, but those fragments failed to interact spontaneously with DMPC vesicles (*21*). Isolation of a 4K fragment of *M. sexta* apoLp-III that consists of the fifth helix displayed a predominantly random-coiled, unstructured state (*20*), and did not bind to DMPC vesicles. From NMR studies with the 4K peptide (*22*) as well as with full-length protein (*13*), it was concluded that hydrophobic interhelical contacts, such as between helix-1 and helix-5 and between helix-2 and helix-5, are necessary for proper folding of apoLp-III. The presence of three complete helices in apoLp-III(1−91) might permit such interhelical contacts.

It is evident that apoLp-III(1−91) is a stable apolipoprotein and retains the ability to associate with lipoproteins and to interact with phospholipid vesicles. Thus, it can be concluded that this deletion mutant, that is composed of helix-1, helix-2 and helix-3, contains the basic structural elements needed for lipid binding. The design and expression of truncated versions of apoLp-III enables investigations of structural elements involved in lipid association to apolipoproteins, but also is useful for study of other physiological functions, such as the role of apoLp-III in regulation of insect immunity (*1*, *7*). The immune stimulating function of apoLp-III might be restricted to the presence of apoLp-III in the lipid-bound form (*8*) although the mechanism of this process remains to be solved. It will be of interest if also the immune stimulating activity is conserved in apoLp-III(1−91). In addition, the relatively small size of the deletion mutant facilitates NMR studies of the lipid-bound protein.

ACKNOWLEDGMENT

We thank Robert Luty for CD analysis, Leslie D. Hicks for performing analytical ultracentrifugation experiments, and Roger Bradley for electron microscopy and photography.

REFERENCES

1. Wiesner, A., Losen, S., Kopácek, P., and Götz, P. (1997) *J. Insect Physiol. 43*, 383−391.
2. Weise, C., Franke, P., Kopácek, P., and Wiesner, A. (1998) *J. Protein Chem. 17*, 633−641.
3. Van der Horst, D. J. (1990) *Biochim. Biophys. Acta 1047*, 195−211.
4. Blacklock, B. J., and Ryan, R. O. (1994) *Insect Biochem. Mol. Biol. 24*, 855−873.
5. Soulages, J. L., and Wells, M. A. (1994) *Adv. Protein Chem. 45*, 371−415.
6. Ryan, R. O., and Van der Horst, D. J. (2000) *Annu. Rev. Entomol. 45*, 231−258.
7. Niere, M., Meisslitzer, C., Dettloff, M., Weise, C., Ziegler, M., and Wiesner, A. (1999) *Biochim. Biophys. Acta 1433*, 16−26.
8. Dettloff, M., and Wiesner, A. (1998) in *Techniques in Insect Immunology* (Wiesner, A., Sugumaran, M., Marmaras, V. J., Morishima, I., Yamakawa, M., and Dunphy, G. B., Eds.) pp 243−251, SOS Publications, Fair Haven, NJ.
9. Sun, D., Ziegler, R., Milligan, C. E., Fahrbach, S., and Schwartz, L. M. (1995) *J. Neurobiol. 26*, 119−129.
10. Dunphy, G. B., and Halwani, A. E. (1997) *J. Insect Physiol. 43*, 1023−1029.
11. Iimura, Y., Ishikawa, H., Yamamoto, K., and Sehnal, F. (1998) *Arch. Insect Biochem. Physiol. 38*, 119−125.
12. Breiter, D. R., Kanost, M. R., Benning, M. M., Wesenberg, G., Law, J. H., Wells, M. A., Rayment, I., and Holden, H. M. (1991) *Biochemistry 30*, 603−608.
13. Wang, J., Gagné, S. M., Sykes, B. D., and Ryan, R. O. (1997) *J. Biol. Chem. 272*, 17912−17920.
14. Wells, M. A., Ryan, R. O., Kawooya, K., and Law, J. H. (1987) *J. Biol. Chem. 262*, 4172−4176.
15. Narayanaswami, V., Wang, J., Kay, C. M., Scraba, D. G., and Ryan, R. O. (1996) *J. Biol. Chem. 271*, 26855−26862.
16. Weers, P. M. M., Kay, C. M., Oikawa, K., Wientzek, M., Van der Horst, D. J., and Ryan, R. O. (1994) *Biochemistry 33*, 3617−3624.
17. Wientzek, M., Kay, C. M., Oikawa, K., and Ryan, R. O. (1994) *J. Biol. Chem. 269*, 4605−4612.
18. Weers, P. M. M., Narayanaswami, V., Kay, C. M., and Ryan, R. O. (1999) *J. Biol. Chem. 274*, 21894−21810.

19. Narayanaswami, V., Wang, J., Schieve, D., Kay, C. M., and Ryan, R. O. (1999) *Proc. Natl. Acad. Sci. U.S.A. 96*, 4366−4371.
20. Narayanaswami, V., Kay, C. M., Oikawa, K., and Ryan, R. O. (1994) *Biochemistry 33*, 13312−13320.
21. Narayanaswami, V., Weers, P. M. M., Bogerd, J., Kooiman, F. P., Kay, C. M., Scraba, D. G., Van der Horst, D. J., and Ryan, R. O. (1995) *Biochemistry 34*, 11822−11830.
22. Wang, J., Narayanaswami, V., Sykes, B. D., and Ryan, R. O. (1998) *Protein Sci. 7*, 336−341.
23. Ryan, R. O., Schieve, D., Wientzek, M., Narayanaswami, V., Oikawa, K., Kay, C. M., and Agellon, L. B. (1995) *J. Lipid Res. 36*, 1066−1072.
24. Laemmli, U. K. (1970) *Nature 227*, 680−685.
25. Babul, J., and Stellwagen, E. (1969) *Anal. Biochem. 28*, 216−221.
26. Johnson, M. L., Correia, J. J., Yphantis, D. A., and Halvorson, H. R. (1981) *Biophys. J. 36*, 575−588.
27. Cohn, E. J., and Edsall, J. T. (1943) in *Proteins, Amino acids and Peptides* (Cohn, E. J., Edsall, J. T., Eds.) pp 370−381, Reinhold Publishing Corp., New York.
28. Provencher, S. W., and Glöckner, J. (1981) *Biochemistry 20*, 33−37.
29. MacDonald, R. C., MacDonald, R. I., Menco, B. P. M., Takeshita, K., Subbarao, N. K., and Hu, L. (1991) *Biochim. Biophys. Acta 1061*, 297−303.
30. Liu, H., Scraba, D. G., and Ryan, R. O. (1993) *FEBS Lett. 316*, 27−33.
31. Singh, T. K. A., Liu, H., Bradley, R., Scraba, D. G., and Ryan, R. O. (1994) *J. Lipid Res. 35*, 1561−1569.
32. Eisenberg, D., Schwarz, E., Komaromy, M., and Wall, R. (1984) *J. Mol. Biol. 179*, 125−142.
33. Ryan, R. O., Oikawa, K., and Kay, C. M. (1993) *J. Biol. Chem. 268*, 1525−1530.
34. Weers, P. M. M., Van der Horst, D. J., and Ryan, R. O. (2000) *J. Lipid Res 41*, 416−423.
35. Kanellis, P., Romans, A. Y., Johnson, B. J., Kercret, H., Chiovetti, R., Jr., Allen, T. M., and Segrest, J. P. (1980) *J. Biol. Chem. 255*, 11464−11472.
36. Zhang, Y., Lewis, R. N. A. H., McElhaney, R. N., and Ryan, R. O. (1993) *Biochemistry 32*, 3942−3952.
37. Soulages, J. L., and Bendavid, O. J. (1998) *Biochemistry 37*, 10203−10210.
38. Wang J., Liu, H., Sykes, B. D., and Ryan, R. O. (1992) *Biochemistry 31*, 8706−8712.
39. Soulages, J. L., Salamon, Z., Wells, M. A., and Tollin, G. (1995*) Proc. Natl. Acad. Sci. U.S.A. 92*, 5650−5654.
40. Soulages, J. L., van Antwerpen, R., and Wells, M. A. (1996) *Biochemistry 35*, 5191−5198.
41. Surewicz, W., Epand, R. M., Pownall, H. J., and Hiu, S.-K. (1986) *J. Biol. Chem. 261*, 16191−16197.
42. Segrest J. P., Jones, M. K., De Loof, H., Brouillette, C. G., Venkatachalapathi, Y. V., and Anantharamaiah, G. M. (1992) *J. Lipid Res. 33*, 141−166.
43. Segrest, J. P., Garber, D. W., Brouillette, C. G., Harvey, S. C., and Anantharamaiah, G. M. (1994) *Adv. Protein Chem. 45*, 303−369.
44. Jonas, A., Steinmetz, A., and Churgay, L. (1993) *J. Biol. Chem. 268*, 1596−1602.
45. Anantharamaiah, G. M., Jones, J. L., Brouillette, C. G., Schmidt, C. F., Chung, B. H., Hughes, T. A., Bhown, A. S., and Segrest, J. P. (1985) *J. Biol. Chem. 260*, 10248−10255.
46. Mishra, V. K., Palgunachari, M. N., Datta, G., Phillips, M. C., Lund-Katz, S., Adeyeye, S. O., Segrest, J. P., and Anantharamaiah, G. M. (1998) *Biochemistry 37*, 10313−10324.

BI0013804